Species interactions in binary particulate systems

J. Liu*
Department of Mechanical Engineering, The Johns Hopkins University, Baltimore, Maryland 21218, USA
and Theoretical Division, Fluid Dynamics Group T-3, B216, Los Alamos National Laboratory, Los Alamos, New Mexico 87545, USA

S. Y. Chen†
Department of Mechanical Engineering, The Johns Hopkins University, Baltimore, Maryland 21218 USA
and CoE and CCSE, Peking University, Beijing, China

D. Z. Zhang‡
Theoretical Division, Fluid Dynamics Group T-3, B216, Los Alamos National Laboratory, Los Alamos, New Mexico 87545, USA
(Received 14 November 2007; revised manuscript received 19 March 2008; published 2 June 2008)

In many models for binary particulate systems, the relative motion between two particle species is modeled by diffusion. Recently, two-equation models have been used to improve diffusion models. While two-equation models are significant improvements to diffusion models and are applicable in modeling dilute systems, they are still theoretically inadequate for dense systems. This inadequacy directly results from the assumption that the species interaction forces in the two momentum equations sum to zero. In fact, the sum of the two forces is not zero but the divergence of an interspecies stress [Zhang, Ma, and Rauenzahn, Phys. Rev. Lett. **97**, 048301 (2006)]. Introduction of this interspecies stress amends the inadequacy in two-equation models. The main objective of the present paper is to examine the importance of this newly introduced interspecies stress relative to other known stresses in the system. For this purpose we numerically simulate the simplest possible granular system. The interspecies stress is of the same order of magnitude as other stresses for dense systems. Additionally, we also examine properties of the species interaction force under different conditions.

DOI: 10.1103/PhysRevE.77.066301 PACS number(s): 47.57.Gc, 47.55.−t, 83.10.Rs, 45.70.Mg

I. INTRODUCTION

Mixing and segregation of binary particulate materials play important roles in many practical engineering applications such as production of pharmaceuticals and ceramics and combustor mixing [1]. This topic has been extensively studied [2–6]. Currently, in many continuum level descriptions, the motion of the involved materials is described by a momentum equation for the mixture. The relative motion of the two different species of particles is often modeled as various diffusion processes [1,2]. This is similar to the drift-flux models used in the early era of two-phase flow theories. In the case of a strong pressure gradient or significant relative motion between phases, two-equation models (also called two-fluid models) have significant advantages over the drift-flux theory in modeling two-phase flows. To improve these mixing models, recently two-equation models have been introduced [7,8] for particulate systems. In these models, the interaction between the two species is solely represented by exchange forces in the momentum equations. Although this type of two-equation model can be derived using the Boltzmann equation for dilute systems [9,10], it is often applied to mixtures of dense particulate systems (such as dense granular flows, dense gases, or even liquids). In these models the sum of exchange forces is regarded as zero on the grounds of the action-and-reaction principle. This is a good approximation for a dilute system but not for dense systems, as demonstrated in [11], because the correct application of the action-and-reaction principle actually leads to an interspecies stress. The sum of the species interaction forces is the divergence of an interspecies stress. In [11], the two-equation model is derived based on the Liouville equation instead of on the Boltzmann equation or its extensions. Therefore, assumptions such as instantaneous binary collisions and molecular chaos, associated with the Boltzmann equation, are not necessary.

The use of the Liouville equation to derive macroscopic equations based on interactions at the particle scale is not new and was used by Irving and Kirkwood [12] to derive the Navier-Stokes equation from molecular interactions. The derivation in [11] extends the method of Irving and Kirkwood to binary systems. The interspecies stress is obtained, similar to the collisional stress in the original derivation. In a dilute system, the collisional and interspecies stresses are unimportant. For dense systems, however, collisional stresses are the dominant fraction; and the interspecies stress also becomes important in the mixture. The importance of the interspecies stress in the total stress of the mixture has been explained, but not its role in the momentum equations in a two-equation model. In a similar fashion, the concept of partial pressure is applicable only to a mixture of ideal gases but not to dense gases. If the interactions of different species could solely be represented by an exchange force appearing in the momentum equation for each of the species, then interspecies interactions would not appear in the mixture momentum equation obtained by summing together the momentum equations for all the species, because the exchange forces sum to zero. One would then conclude that the con-

*jliu36@jhu.edu
†syc@jhu.edu
‡Corresponding author. dzhang@lanl.gov

cept of partial pressure is correct for mixtures of dense gases as well, because the only stress in the mixture momentum equation is the sum of the stresses of the individual species. This, of course, cannot be correct. If we divided a system of identical particles into two species in some arbitrary manner, the interactions between particles belonging to different species would have no contribution to the total stress calculated in this way. In other words, some of the particle interactions would be excluded from the total stress depending on the arbitrary division. On the other hand, if the total stress is calculated without such division, then the total stress includes effects of all particle interactions. The only way to resolve this paradox is to include a stress representing interspecies interactions in the total stress; and this stress must be present in the momentum equation for each species.

Another issue related to the species momentum equations is the form of the averaged equations. If we regard a disperse two-phase flow as a limit of a binary mixture in which a large number of small particles, such as water molecules surrounding a relatively smaller number of large particles, say salt grains, a correct two-equation model for the binary particulate system should reduce to the equations for disperse two-phase flows in this limit. The commonly used momentum equations [7–10] for binary particulate systems have the volume fraction, or the particle number density, inside the divergence, while it is now well accepted that for disperse two-phase flows, the volume fraction should appear outside the divergence of the stress [13–15]. Both forms of the equations are correct in the flow regions for which they are derived. However, if one studies the transition between a disperse two-phase flow to a molecular mixture, for instance, dissolution of salt grains in water, a unified framework of equations is necessary for a smooth transition between these two flow situations. This transition is possible only with the presence of the interspecies stress in the momentum equations [11].

The main objective of the present paper is to study the properties of the interspecies stress using direct numerical simulations. To focus on the basic physics associated with this stress and to avoid introducing effects of other less essential mechanisms, we choose to numerically simulate the simplest possible binary particulate system. The system consists of particles of unit radius and mass of two different species, which are painted with different colors with no dynamic significance. Particles do not interact with each other until they are in contact. During a contact the force between the pair of particles is in the normal direction and linearly proportional to their combined deformation. The tangential force is not considered. Although this is a highly idealized system, we choose to study it first to ensure that the behavior of the stresses and the interaction force is not caused by any difference in the physical properties. The results obtained from this system should provide a baseline for study of more complicated practical systems.

The method of numerical simulation is the discrete element method. This type of method is deemed as the most straightforward approach if the interaction between the particles is known. Although for a practical system choosing a correct force model for particle interaction could be a significant modeling issue; for the purpose of this paper the linear force model is sufficient. The numerical method and comparison to kinetic theories have been published previously [16–18]. In the present paper, we describe only the implementation of the related numerical steps needed for our calculations.

II. TWO-EQUATION FORMULATION FOR A BINARY SYSTEM

For a binary system consisting of two species, let $n^{(i)}$ be the number density for species i particles ($i=1,2$). The mass density of the species can be calculated as $\rho^{(i)}=n^{(i)}\overline{m^{(i)}}$, where $\overline{m^{(i)}}$ is the average mass of species i particles, and the overbar denotes the ensemble average. The averaged continuity and momentum equations can be derived by taking appropriate moments of the Liouville equation [11]. The resulting averaged continuity equation is

$$\frac{\partial \rho^{(i)}}{\partial t} + \nabla \cdot (\rho^{(i)} \tilde{\boldsymbol{v}}^{(i)}) = 0, \tag{1}$$

where $\tilde{\boldsymbol{v}}^{(i)}=\overline{m^{(i)}\boldsymbol{v}^{(i)}}/\overline{m^{(i)}}$ is the Favre average of the particle velocity $\boldsymbol{v}^{(i)}$ of species i. The averaged momentum equation is

$$\frac{\partial \rho^{(i)} \tilde{\boldsymbol{v}}^{(i)}}{\partial t} + \nabla \cdot (\rho^{(i)} \tilde{\boldsymbol{v}}^{(i)} \tilde{\boldsymbol{v}}^{(i)}) = \nabla \cdot (\theta^{(i)} \boldsymbol{\sigma}^{(ii)} + \rho^{(i)} \boldsymbol{M}^{(i)}) + n^{(i)} \overline{\boldsymbol{f}^{(ij)}} + \rho^{(i)} \boldsymbol{b}, \tag{2}$$

where $\theta^{(i)}$ is the volume fraction of species i particles, $\boldsymbol{\sigma}^{(ii)}$ is the stress resulting from intraspecies interactions, $n^{(i)}\overline{\boldsymbol{f}^{(ij)}}$ is the force resulting from interspecies interactions, $\rho^{(i)}\boldsymbol{b}$ is the body force, and

$$\rho^{(i)} \boldsymbol{M}^{(i)} = -n^{(i)} \overline{m^{(i)} (\boldsymbol{v}^{(i)} - \tilde{\boldsymbol{v}}^{(i)})(\boldsymbol{v}^{(i)} - \tilde{\boldsymbol{v}}^{(i)})} \tag{3}$$

is the stress resulting from velocity fluctuations.

As shown in [11], the interaction forces $n^{(i)}\overline{\boldsymbol{f}^{(ij)}}$ acting on all the species do not sum to zero. Instead, they sum to the divergence of an interspecies stress $\theta^{(i)}\boldsymbol{\sigma}^{(ij)}$,

$$n^{(1)} \overline{\boldsymbol{f}^{(12)}} + n^{(2)} \overline{\boldsymbol{f}^{(21)}} = \nabla \cdot (\theta^{(i)} \boldsymbol{\sigma}^{(ij)}), \quad i \neq j, \tag{4}$$

where $\theta^{(i)}\boldsymbol{\sigma}^{(ij)}=\theta^{(j)}\boldsymbol{\sigma}^{(ji)}$. Summing the momentum equation (2) over all the species, we find the following mixture momentum equation:

$$\frac{\partial \rho^{(m)} \tilde{\boldsymbol{v}}^{(m)}}{\partial t} + \nabla \cdot (\rho^{(m)} \tilde{\boldsymbol{v}}^{(m)} \tilde{\boldsymbol{v}}^{(m)}) = \rho^{(m)} \boldsymbol{b} + \nabla \cdot \boldsymbol{\sigma}^{m}, \tag{5}$$

where $\rho^{(m)}=\theta^{(1)}\rho^{(1)}+\theta^{(2)}\rho^{(2)}$ is the mixture density and $\boldsymbol{\sigma}^{m}$ is the mixture stress defined as

$$\boldsymbol{\sigma}^{m} = \rho^{(1)} \boldsymbol{M}^{(1)} + \rho^{(2)} \boldsymbol{M}^{(2)} + \frac{\rho^{(1)} \rho^{(2)}}{\rho^{(m)}} \boldsymbol{M}^{(12)} + \theta^{(1)} \boldsymbol{\sigma}^{(11)} + \theta^{(2)} \boldsymbol{\sigma}^{(22)} + \theta^{(1)} \boldsymbol{\sigma}^{(12)}, \tag{6}$$

with $\boldsymbol{M}^{(12)}=-(\tilde{\boldsymbol{v}}^{1}-\tilde{\boldsymbol{v}}^{2})(\tilde{\boldsymbol{v}}^{1}-\tilde{\boldsymbol{v}}^{2})$. The stress $\rho^{(1)}\rho^{(2)}\boldsymbol{M}^{(12)}/\rho^{(m)}$ results from the average relative motion between the species. This term can be viewed as a result of velocity fluctuations in the average species velocity relative to the mean mixture velocity. Thus, there are two distinct contributions to the

mixture stress: one from velocity fluctuations represented by the $\boldsymbol{M}$ terms, and the other from the particle interactions represented by the $\boldsymbol{\sigma}$ terms. The mixture stress contains not only the intraspecies interactions but also the interspecies interactions. In a dilute system, contributions from particle interactions can be neglected. If the relative motion between the species is also negligible, the mixture stress is then the sum of the stresses, $\rho^{(i)}\boldsymbol{M}^{(i)}$, of both species. In this case the concept of partial stress or partial pressure applies. When the particle interactions are important, the stress on each species can be defined as

$$\boldsymbol{\sigma}^{(i)} = \rho^{(i)}\boldsymbol{M}^{(i)} + \theta^{(i)}\boldsymbol{\sigma}^{(ii)}. \tag{7}$$

However, with this definition, the mixture stress cannot be expressed as a sum of the stresses of the individual species because the interspecies stress $\theta^{(i)}\boldsymbol{\sigma}^{(ij)}$ is as important as the intraspecies stress $\theta^{(i)}\boldsymbol{\sigma}^{(ii)}$, as shown in Sec. IV. Indeed, the concept of partial pressure does not apply to dense gases and liquids.

The momentum equation for each species can be written in a symmetric form by introducing the species exchange force $\boldsymbol{F}^{(ij)}$ such that

$$n^{(i)}\boldsymbol{f}^{(ij)} = \boldsymbol{F}^{(ij)} + \theta^{(i)}\nabla\cdot(c_i\boldsymbol{\sigma}^{(ij)}) + c_j\boldsymbol{\sigma}^{(ji)}\cdot\nabla\theta^{(j)}, \tag{8}$$

where $\boldsymbol{F}^{(ij)}=-\boldsymbol{F}^{(ji)}$, and c_i and c_j, satisfying $c_1+c_2=1$, are partitioning coefficients depending on the particle system. For instance, for disperse two-phase flows, if species 1 is the continuous phase; and species 2 is the disperse phase, by comparing (8) to relation (21) in [11] and using (22) in that paper, we find $c_1=0$, $c_2=1$, and $\boldsymbol{F}^{(21)}=\theta^{(2)}(\boldsymbol{A}^{(21)}-\nabla\cdot\boldsymbol{T}^{(21)})$, where $\boldsymbol{A}^{(21)}$ and $\boldsymbol{T}^{(21)}$ are the phase interaction force and the phase interaction stress [11,13,14]. By using these results, the averaged equations for disperse two-phase flow are recovered. For systems simulated in this paper, c_1 and c_2 are equal to 1/2, because of the identical nature of the particle species.

With relation (8), the species momentum equation (2) can be written in a symmetric form as

$$\frac{\partial\rho^{(i)}\tilde{\boldsymbol{v}}^{(i)}}{\partial t} + \nabla\cdot(\rho^{(i)}\tilde{\boldsymbol{v}}^{(i)}\tilde{\boldsymbol{v}}^{(i)}) = \nabla\cdot\boldsymbol{\sigma}^{(i)} + \boldsymbol{F}^{(ij)} + \theta^{(i)}\nabla\cdot(c_i\boldsymbol{\sigma}^{(ij)}) + c_j\boldsymbol{\sigma}^{(ji)}\cdot\nabla\theta^{(j)} + \rho^{(i)}\boldsymbol{b}. \tag{9}$$

Closure relations for the stresses and the species exchange force are needed to close the equation system. Finding general closure relations for them is a significant challenge and is beyond the scope of this work. The main objective of this paper is to study their properties and behaviors in a few idealized cases as a starting point to explore general closure relations for practical problems.

III. CALCULATION OF THE FORCE AND THE STRESSES

The species interaction force mentioned in the previous section is an ensemble-averaged quantity [11]. For particle systems with finite degrees of freedom, let $\mathcal{C}$ be the set of parameters, called the configuration, uniquely describing a system. These configurations or parameter sets constitute a phase space. Let $P(\mathcal{C},t)$ be the probability density defined in this phase space, such that the probability of finding a configuration in the vicinity, $d\mathcal{C}$, of configuration $\mathcal{C}$ can be calculated as $d\mathcal{P}=P(\mathcal{C},t)d\mathcal{C}$. At a specified location $\boldsymbol{x}$ and time t, the averaged species interaction force is related to particle interaction forces in the system by [11]

$$n^{(i)}(\boldsymbol{x},t)\overline{\boldsymbol{f}^{(ij)}}(\boldsymbol{x},t) = \int\sum_{\alpha=1}^{N^{(i)}}\delta(\boldsymbol{y}_\alpha^{(i)}-\boldsymbol{x})\sum_{\gamma=1}^{N^{(j)}}\boldsymbol{f}_{\alpha\gamma}^{ij}(\mathcal{C},t)d\mathcal{P} \quad (i\neq j), \tag{10}$$

where $\boldsymbol{f}_{\alpha\gamma}^{ij}$ is the force applied by particle γ of species j on particle α of species i located at $\boldsymbol{y}_\alpha^{(i)}$. Although in many numerical models for particle interaction forces, including the one used in this paper, the interaction force $\boldsymbol{f}_{\alpha\gamma}^{ij}$ depends only on the relative positions of the interacting pair, in many physical systems the particle interaction force can also depend on the positions and states of the neighboring particles. For generality, the force is treated as a function of the configuration $\mathcal{C}$ in [11]. Similarly, the stress is also an ensemble-averaged quantity defined as

$$\theta^{(i)}(\boldsymbol{x},t)\boldsymbol{\sigma}^{(ij)}(\boldsymbol{x},t) = (1-\delta_{ij}/2)\int\sum_{\alpha=1}^{N^{(i)}}\delta(\boldsymbol{y}_\alpha^{(i)}-\boldsymbol{x})\times\sum_{\gamma=1}^{N^{(j)}}\boldsymbol{f}_{\alpha\gamma}^{(ij)}(\mathcal{C},t)(\boldsymbol{y}_\gamma^{(j)}-\boldsymbol{y}_\alpha^{(i)})d\mathcal{P}, \tag{11}$$

where $\boldsymbol{y}_\gamma^{(j)}$ is the location of particle γ of species j.

The averaged equations mentioned in the last section and expressions (10) and (11) for the interaction force and stress are derived in [11] under the assumption that the particle systems have finite degrees of freedom. Although in all the examples discussed in the present paper this assumption is correct, we note that it can be lifted. All the equations and the expressions in [11] and those so far listed in this paper are also correct for particulate systems with infinite degrees of freedom. The only change needed to rederive them for systems with infinite degrees of freedom is to use an abstract and description-independent probability on the average and the probability integrals appearing in the expressions. Since systems of infinite degrees of freedom are not a subject of this paper, we will not discuss this issue further. Readers interested in this subject are referred to Appendix A of [19] for details.

A rigorous calculation of the ensemble-averaged quantities defined in (10) and (11) requires one to calculate many systems with the same macroscopic conditions and then average over them. In the numerical calculation of the species interaction forces and stresses, we consider a statistically homogeneous distribution of particles in a cube of volume V with periodic boundaries. For such a system, the species exchange force $\boldsymbol{F}^{(ij)}$, defined in (8), is identical to the species interaction force $n^{(i)}\overline{\boldsymbol{f}^{(ij)}}$. For each initial configuration in our numerical simulation, statistical data are collected after the system reaches a statistical steady state. The species exchange force and the stresses are calculated as volume- and time-averaged quantities. In this way, the force and the stress can be calculated as

$$\boldsymbol{F}^{(ij)}(\boldsymbol{x},t) = n^{(i)}(\boldsymbol{x},t)\overline{\boldsymbol{f}^{(ij)}}^{\mathrm{IC}}(\boldsymbol{x},t) = \frac{1}{\tau_a V}\int \sum_{\alpha=1}^{N^{(i)}}\sum_{\gamma=1}^{N^{(j)}} \boldsymbol{f}_{\alpha\gamma}^{ij} dt \qquad (i \neq j) \tag{12}$$

and

$$\theta^{(i)}(\boldsymbol{x},t)\boldsymbol{\sigma}^{(ij)}(\boldsymbol{x},t) = (1-\delta_{ij}/2)\overline{\frac{1}{\tau_a V}\int \sum_{\alpha=1}^{N^{(i)}}\sum_{\gamma=1}^{N^{(j)}} \boldsymbol{f}_{\alpha\gamma}^{ij}(\boldsymbol{y}_{\gamma}^{(j)} - \boldsymbol{y}_{\alpha}^{(i)}) dt}^{\mathrm{IC}}, \tag{13}$$

where τ_a is the time interval for the time average, the summations are over all interacting pairs between species i and species j particles, and the overbar with "IC" denotes the average over all possible initial configurations.

In our numerical simulations, the temporally and spatially averaged values of the force and the stresses do not vary significantly with different initial particle configurations; therefore it is not necessary to average over different initial particle configurations as suggested in (12) and (13). Most values reported in this paper are obtained by temporal and spatial averaging over a single initial particle configuration. Simulations using different initial particle configurations are performed only for a few selected macroscopic conditions to ensure that there are no significant differences in the values of the force and the stresses.

The initial particle configurations are generated using the method suggested by Ma and Zhang [20]. 2048 particles are first placed into a large enough periodic box according to a fcc structure. Then each particle is given 5000 chances for random movement with a mean displacement equal to the mean free path. Only movements that do not result in particle overlap are accepted. Afterward, the simulation domain is shrunk slowly and uniformly in all three directions until the volume fraction reaches the specified value; then the domain is expanded to a larger volume uniformly in all directions to allow the stresses to relax to zero before it is shrunk again. The stress in the shrunken state is reduced during these contraction-expansion cycles. After enough such cycles, the stress at the contracted state reaches a small enough value, and the particle configuration is accepted as the initial condition. This process ensures that the resulting configurations are statistically homogeneous and the fcc structures associated with the initial configurations are destroyed even with very dense particulate systems. After this process, particles are assigned randomly to two species according to the ratio of their number densities.

The two-equation formulation described above applies equally well to molecular systems and granular systems. In the present paper we simulate granular systems in which particles are spheres with equal radius a and mass m. Particles interact only during a collision, in which the interaction force is assumed to be in the normal direction and is given by

$$f_n = K_n(r-2a), \tag{14}$$

where K_n is a coefficient and r is the distance between the particle centers. This is an idealized linear force model that does not dissipate energy. While the numerical tool used in this calculation is capable of studying more general and practical granular flows [17,20,21], the main objective of the present paper is to explore the species interaction force and the stresses in the simplest possible system. To avoid additional complications due to energy dissipation, we intentionally use this linear force model. This choice is similar to the use of a unit restitution coefficient in early kinetic theories of granular flows [22,23].

The average velocity of species 1 is initially zero; and the average velocity of species 2 is set to the specified relative velocity between the two species. The initial particle velocity is the sum of the average species velocity and a fluctuation component. The fluctuation component of the particle velocity has a zero mean and obeys the Gaussian distribution with a specified granular temperature defined as

$$T^{(i)} = \frac{1}{3N^{(i)}}\sum_{\alpha=1}^{N^{(i)}} m(\boldsymbol{v}_{\alpha}^{(i)} - \tilde{\boldsymbol{v}}^{(i)})^2, \tag{15}$$

where $N^{(i)}$ is the total number of particles for species i, m is the particle mass, $\boldsymbol{v}_{\alpha}^{(i)}$ is the velocity for particle α of species i, and $\tilde{\boldsymbol{v}}^{(i)}$ is the average velocity,

$$\tilde{\boldsymbol{v}}^{(i)} = \sum_{\alpha=1}^{N^{(i)}} \boldsymbol{v}_{\alpha}^{(i)}/N^{(i)}. \tag{16}$$

In the simulations, all physical quantities are nondimensionalized. The length is nondimensionalized by the particle radius a, the mass is nondimensionalized by the particle mass m, and the time scale is chosen such that $200\sqrt{m/K_n}$ is the time of unity, which implies $K_n = 40\,000$. To provide a connection between these numerical simulations and practical systems, let us now suppose the particles are fine sand grains about 100 μm in diameter. It is estimated [18] that the binary collision time of the grains is of order 10 μs, the time unit in our simulation (or $200\sqrt{m/K_n}$) is about 0.5 ms, and the velocity unit is about 0.1 m/s in the system of sand grains.

The evolution of particle positions is solved directly from the equations of motion for the particles [17,18] using an explicit second-order leapfrog time scheme. The time step is set to be a few percent of the natural period of the mass-spring model (14) for particle interactions,

$$\Delta t = 0.03\sqrt{\frac{m}{2K_n}}. \tag{17}$$

For the force model (14) used in the simulation the total energy per particle can be calculated as

$$E_{\mathrm{total}} = \frac{1}{N}\sum_{i=1}^{N}\frac{1}{2}m_i v_i^2 + \frac{1}{N}\sum_{p}\frac{1}{2}K_n(r-2a)^2, \tag{18}$$

where N is the total number of particles in the system for both species, r is the distance between the centers of a contacting pair, and Σ_p denotes the summation over all contacting pairs. Since the force model (14) is conservative, the total energy is a constant if no external force is applied to the system. Energy conservation is verified numerically in our simulation.

For cases studied in the second part of the next section where two species experience a relative mean motion, an external force is needed to maintain a constant relative velocity. For these cases, we study the species interaction force and the stresses as functions of the temperature or the kinetic energy associated with velocity fluctuations. To ensure a constant temperature in such a simulation, the granular temperature is rescaled every time step using the following method commonly employed in many molecular dynamics simulations [16]. At each time step, the granular temperature $T^{(i)}$ for each species is calculated according to (15). The velocity $\boldsymbol{v}_\alpha^{(i)}$ for particle α is then replaced by

$$\tilde{\boldsymbol{v}}^{(i)} + \sqrt{\frac{T_s^{(i)}}{T^{(i)}}}(\boldsymbol{v}_\alpha^{(i)} - \tilde{\boldsymbol{v}}^{(i)}), \tag{19}$$

so that the granular temperature in the system equals the specified value $T_s^{(i)}$. In this rescaling procedure, only the fluctuation component of the velocity is altered and the mean velocity remains unchanged. This is equivalent to applying random body forces with zero mean to particles to supply to or extract energy from the system such that the temperature in the system stays constant. In the calculations performed for the present work the specified granular temperatures are the same for both species.

To maintain the mean velocity at a specified value $\boldsymbol{U}^{(i)}$ during the calculations, at the end of each time step the discrepancy $\boldsymbol{U}^{(i)} - \tilde{\boldsymbol{v}}^{(i)}$ between the specified velocity $\boldsymbol{U}^{(i)}$ and the average velocity defined in (16) is added to each particle, and the velocity for particle α is reset to

$$\boldsymbol{v}_\alpha^{(i)} + \boldsymbol{U}^{(i)} - \tilde{\boldsymbol{v}}^{(i)}. \tag{20}$$

This procedure is equivalent to applying uniform body forces to particles to maintain the mean velocity of the species regardless of any interaction forces between species.

IV. RESULTS AND DISCUSSION

In this section, we first present an example at thermal equilibrium to examine the relative importance of interspecies stresses $\theta^{(1)}\boldsymbol{\sigma}^{(12)}$ in the mixture stress $\boldsymbol{\sigma}^m$ defined in (6), and then study cases with a relative motion between species.

A. Granular system without relative motion between species

After initial particle positions are generated as described in the previous section, we evenly and randomly label half of the particles as species 1, the rest as species 2. We assign a random velocity to each particle according to the Gaussian distribution. To ensure zero mean velocity, we then calculate the mean velocity of the particle system and use (20) to reset particle velocities.

Because there is no relative average velocity between species, the term $\rho^{(1)}\rho^{(2)}\boldsymbol{M}^{(12)}/\rho^{(m)}$ in (6) vanishes. Since the system studied in this case is isotropic, the stress defined in (6) is statistically isotropic and the pressure $p = -\sigma_{xx} = -\sigma_{yy} = -\sigma_{zz}$. Because of fluctuations in the simulations, the nondiagonal components in the stresses are not exactly zero but are negligibly small compared to the diagonal elements. Also there are slight differences in the diagonal elements as well. The pressure is calculated from the average of the three diagonal elements. Figure 1 shows the ratio of the interspecies stress to the mixture stress at two nondimensional temperatures 100 and 10 000, corresponding to about 1.7 and 17 m/s fluctuating velocity for the fine sand particles mentioned in the previous section. This ratio of the interspecies stress to the mixture stress increases with total volume fraction, $\theta^{(m)} = \theta^{(1)} + \theta^{(2)}$, and decreases with temperature. In other words, the interspecies stress formulated in [11] is important in dense, slow, particulate systems and less so in rapid and dilute particulate systems. This partially explains why the interspecies stress was not well studied in kinetic theories for dilute systems. In this simulation, the particle numbers and properties of the two species are identical. In this system, every particle has the same chance of contacting a particle of its own species or a particle of the other species; therefore $\theta^{(1)}\sigma^{(12)} = 2\theta^{(1)}\sigma^{(11)} = 2\theta^{(2)}\sigma^{(22)}$. If this system is at the limit of zero temperature and densely packed, the stresses associated with velocity fluctuation in (6) vanish and the mixture stress is then the sum of the particle interaction stresses. Therefore the ratio $\theta^{(1)}\sigma^{(12)}/\sigma^m$ becomes exactly 1/2. For the system with low temperature and high volume fraction simulated in this work, this ratio reaches 0.47 as shown in Fig. 1.

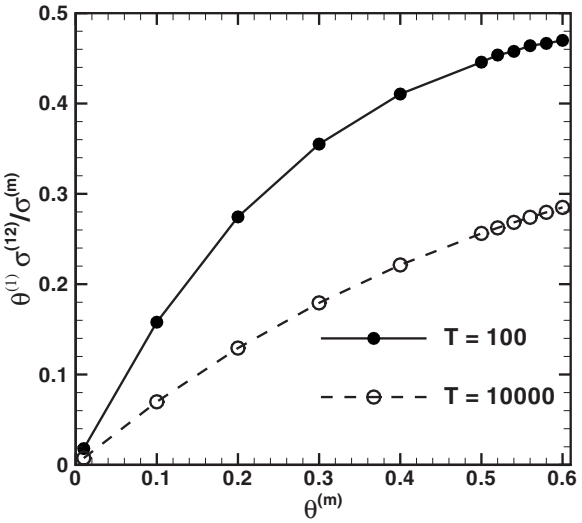

FIG. 1. Ratio of interspecies stress to the mixture stress as function of the total volume fraction $\theta^{(m)}$ for different temperatures. The volume fractions for the two species are the same in this figure.

As shown in [18,21], for slow and dense particulate systems, the time scales of particle interactions have a significant effect on the stress. This suggests that there is an interesting relation between this interspecies stress and the time scales of the particle interactions. This will be a subject for future studies.

B. Granular flow With relative motion

Interactions of a single object immersed in a granular material and in a molecular fluid have been studied by many researchers [24–27]. These studies are focused on the interaction forces on an individual object, except in [28] where

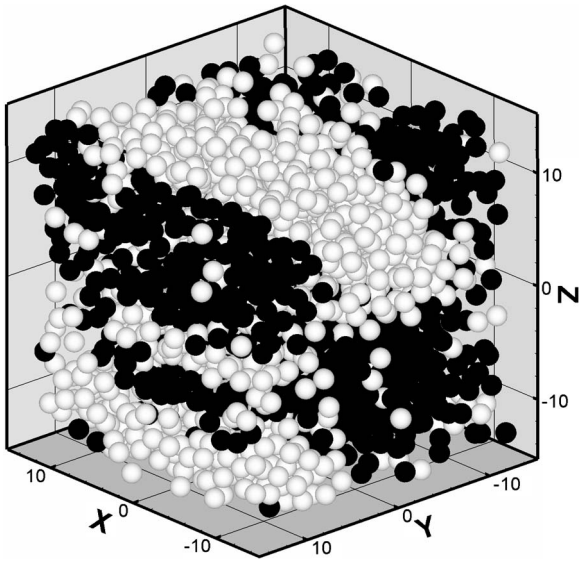

FIG. 2. Segregation introduced by relative motion in the x direction at temperature $T=100$, relative velocity $U=20$, and volume fractions $\theta^{(1)}=\theta^{(2)}=0.2$.

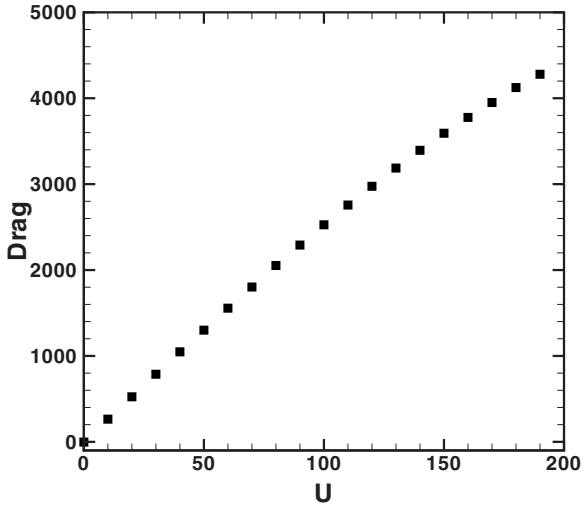

FIG. 3. Average drag on a particle vs relative velocity at granular temperature of 10 000. $\theta^{(1)}=\theta^{(2)}=0.2$.

interaction of a pair of spheres in a rarefied gas is calculated. To study the species interaction force in a two-equation formulation, multiparticle interactions, both intraspecies and interspecies, need to be considered, especially for dense particulate systems. In the present work, numerical simulations are performed to study the multiparticle interactions between different species.

In the following examples, we study the species interaction force and the stresses in particulate systems consisting of two species undergoing a constant relative motion. In the numerical simulation, the initial particle configuration is generated as described in the previous section. The temperature and the relative velocity between the two species are kept constant during the simulation using the velocity rescaling schemes (19) and (20). The simulation results show that, when the granular temperature is low, relative motion introduces species segregation as shown in Fig. 2. In this figure the particles form channels to reduce resistance when passing each other. While this relative-motion-induced segregation by itself is an interesting subject, in the present work we focus on the constitutive properties of the particulate system. The inhomogeneity resulting from the segregation invalidates the method of calculating the species interaction force and the stresses using (12) and (13), and an ensemble average, which requires a large number of simulations, needs to be carried out. To assess the homogeneity of the system in our calculation, the Lacey mixing index is monitored. To calculate the index we divide the computational domain into $N_\ell=5\times5\times5$ cells (five cells in each direction). The particle ratio variance of species i is calculated as [29]

$$S^2=\frac{1}{N}\sum_{k=1}^{N_\ell}N_k(N_k^{(i)}/N_k-r^{(i)})^2, \tag{21}$$

where N is the total number of particles in the system, N_k is the number of particles in cell k, N_k^i is the number of species i particles, and $r^{(i)}$ is the intended particle ratio, which is 1/2 in our simulations. The Lacey mixing index is calculated as

$$M=\frac{S_0^2-S^2}{S_0^2-\overline{S_r^2}}, \tag{22}$$

where $S_0^2=r^{(i)}(1-r^{(i)})$ is the value of S^2 when the particles are completely segregated, and $\overline{S_r^2}$ is $S_r^2=r^{(i)}(1-r^{(i)})/N_k$ averaged over the cells. The value of S_r^2 in cell k is calculated by assuming that N_k particles in the cell are randomly assigned to species i according to probability $r^{(i)}$. For a binary system, since $r^{(1)}+r^{(2)}=1$ and $N_k^{(1)}+N_k^{(2)}=N_k$, the Lacey mixing index is the same when calculated with i chosen to be 1 or 2. For a completely segregated system, the Lacey mixing index $M=0$; and for perfectly mixed system, $M=1$. All the results presented (except Fig. 2) in this paper are obtained from systems with the Lacey mixing index greater than 0.95, and therefore very close to a homogeneous system.

Figure 3 shows the interspecies exchange force $\boldsymbol{F}^{(ij)}$ as a function of the relative velocity U. Since this interaction force is calculated with a constant relative velocity and the system is statistically steady, it can be regarded as drag between the two species. The results shown in Fig. 3 are calculated at a dimensionless granular temperature 10 000, or a dimensionless mean fluctuation velocity 173. In this system the sound speed is of the same order as the mean fluctuation velocity. Figure 3 shows that, for a small Mach number, the ratio between the relative velocity and the sound speed, the drag is proportional to the relative velocity as in a viscous flow. At higher relative velocities, the drag force increases at a rate that is less than linear. While our results at low velocities are in qualitative agreement with the experimental results for a single object immersed in a fluidized granular bed [30], caution is advised when making such a comparison. There are three significant differences between the drag calculated in the present work and the drag measured experimentally. The first difference is the size ratio. In most experimental work, the size of the immersed body is significantly larger than the granular particle, while in this work, the sizes

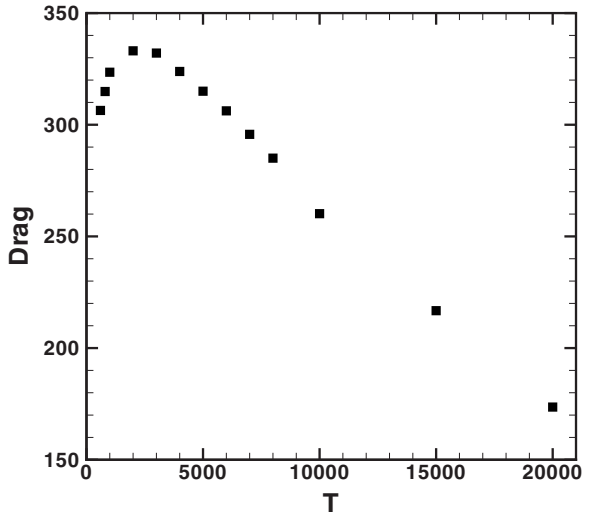

FIG. 4. Averaged drag on a particle vs granular temperature at fixed relative velocity of 10. $\theta^{(1)}=\theta^{(2)}=0.2$.

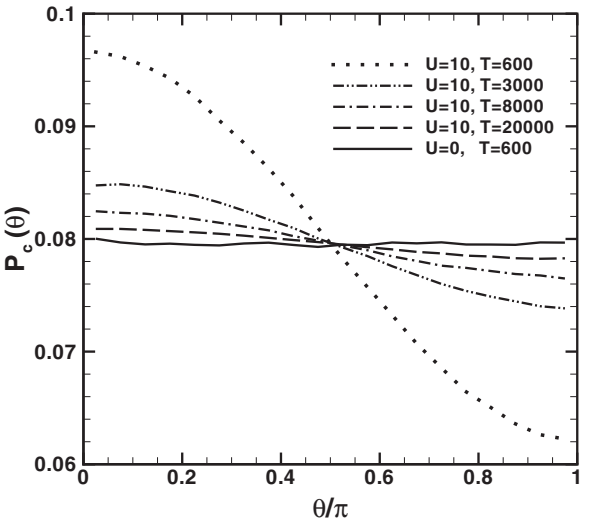

FIG. 5. Contact distribution of species 1 particles on the surface of a species 2 particle at relative velocity 10.

of the particles of the two species are the same. The second major difference concerns multiparticle interactions within the same species. Most reported granular drag forces are measured or calculated for a single object immersed in granular flows. If we view the object as a species, then the object interacts only with particles of the other species. In our simulations, there are many particles in both species, and interactions among particles of the same species are inevitable. Third, unlike in other work, in our simulations, friction is not considered because of the force model used. The stick-and-friction motion observed in [31] is closely related to particle contact time scales [21] that lead to a weak dependence of drag on relative velocity. Although there is no fundamental technical difficulty to include effects of friction in our calculation, to focus on basics of species interactions we decide not to include additional parameters associated with this energy dissipation in the present paper. In this sense, the systems simulated in this work are more similar to dense molecular fluids rather than granular media.

Figure 4 shows the interspecies drag as a function of the granular temperatures at nondimensional velocity 10. As illustrated, the drag first increases with the granular temperature to a maximum value and then decreases as the granular temperature further increases. This indicates that there are at least two competing factors affecting the drag as granular temperature increases. The first factor is similar to the dependence of gas viscosity on temperature. As temperature increases, the collision among the particles increases and results in more efficient momentum transfer and higher viscosity. Therefore the interspecies drag increases. The second factor is related to the asymmetry introduced by relative motion of the species. To quantify this asymmetry, we now introduce the relative density P_c of interspecies contacts on a particle surface defined as follows. For a given solid angle element dS, $N_c P_c dS$ is the number of interspecies contacts within this solid angle element, where N_c is the total number of interspecies contacts on the entire surface. The flow simulated in this paper is statistically axisymmetric about the axis in the flow direction; therefore the relative contact density is only a function of the angle θ from the upwind direction. In Fig. 5 we plot the relative density P_c of interspecies contacts for different granular temperatures. When there is no relative motion between the species, the relative contact density is a constant $(1/4\pi)$. As a reference, we also plot this density calculated in our simulation in the figure as the solid black line. For the cases where a relative velocity between the species is present, this density is maximum in the upwind direction $(\theta=0)$ and minimum in the downwind direction $(\theta=\pi)$ as shown in Fig. 5, indicating the accumulation of particles in the upwind direction and a relative depletion or rarefaction of particles in the downwind direction. As temperature increases, both accumulation and rarefaction are mitigated as shown in the figure. This can be explained by enhanced diffusion at higher temperatures. The reduction of the accumulation and rarefaction reduces the asymmetry introduced by the relative motion and therefore reduces the drag between the species as shown in Fig. 4.

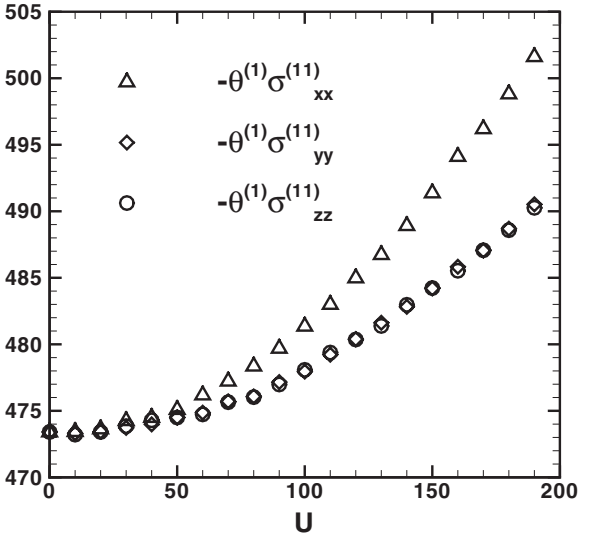

FIG. 6. Intraspecies contact stresses vs relative velocity at granular temperature 10 000. $\theta^{(1)}=\theta^{(2)}=0.2$.

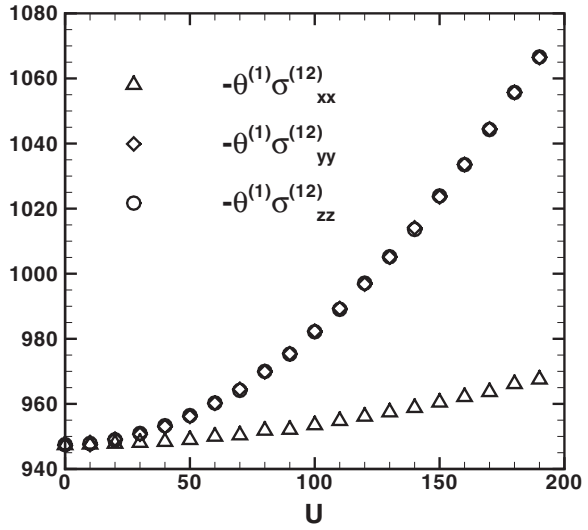

FIG. 7. Interspecies stresses vs relative velocity at granular temperature of 10 000. $\theta^{(1)}=\theta^{(2)}=0.2$.

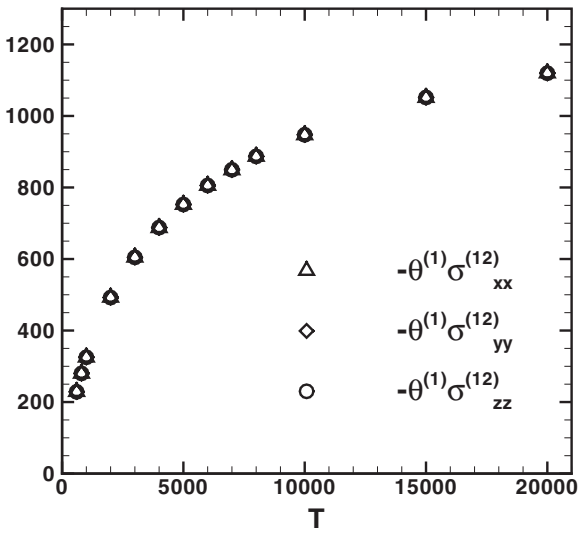

FIG. 9. Interspecies stresses vs granular temperature at fixed relative velocity 10. $\theta^{(1)}=\theta^{(2)}=0.2$.

To explain the reduction of the drag caused by temperature increase we also explore other reasons. Among them, the effect of particle deformations is worth some discussion. From the nondimensionalization scheme described in the previous section. The drag force is nondimensionalized by $K_n a/40\,000$, the temperature is nondimensionalized by $K_n a^2/120\,000$, and velocity is nondimensionalized by $a\sqrt{K_n/m}/200$. Therefore the particle stiffness K_n alone cannot be a reason for the reduction of the drag caused by temperature increase, because both the drag force and the temperature are proportional to K_n. Particle deformation can be caused by both random motion and the relative motion between particles. The deformation caused by relative velocity 100 is comparable to the deformation caused by random motion at temperature 3300 since the kinetic energies associated with these motions are about the same. At this relative velocity the drag is almost proportional to the relative velocity as shown in Fig. 3, while the drag starts to decrease with the temperature at this temperature as shown in Fig. 4. This suggests that drag reduction caused by temperature increase is related to the nature of random motion or diffusion, rather than to the particle deformation.

Figures 6 and 7 show the results of the intraspecies contact stresses and the interspecies stress as functions of the relative velocity. Although the stress change due to the relative velocity is small compared to the background stress, it does not imply that the effect of the relative motion is unimportant. First, the stresses appear on the momentum Eq. (9) under the divergence indicating that the difference in the stress is crucial but not the background stress. For instance, in the case of a pair of spheres moving at the same velocity 100 m/s relative to the air, the pressure change due to the Bernoulli effect can be estimated to be 6000 Pa, only 6% of the atmosphere pressure of 1.0×10^5 Pa. If the two spheres

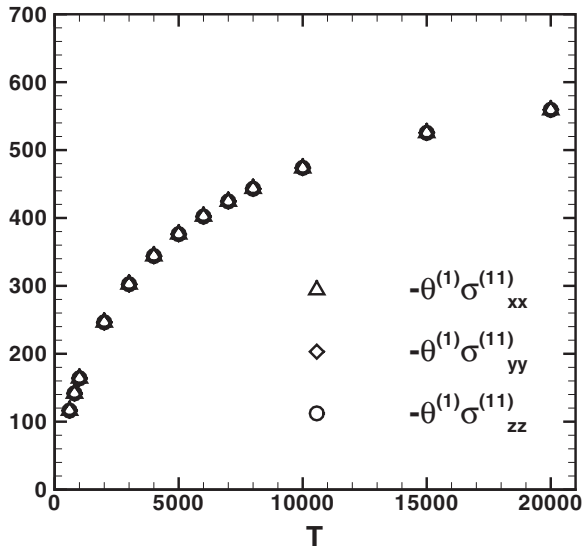

FIG. 8. Intraspecies contact stresses vs granular temperature at fixed relative velocity 10. $\theta^{(1)}=\theta^{(2)}=0.2$.

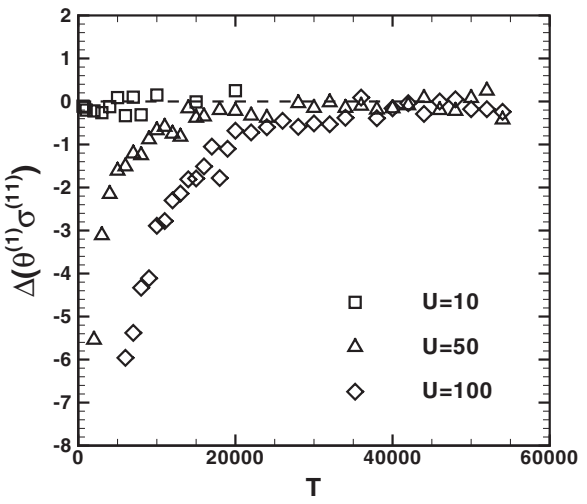

FIG. 10. Intraspecies contact stress difference between the flow direction and the perpendicular directions as a function of granular temperature. $\theta^{(1)}=\theta^{(2)}=0.2$.

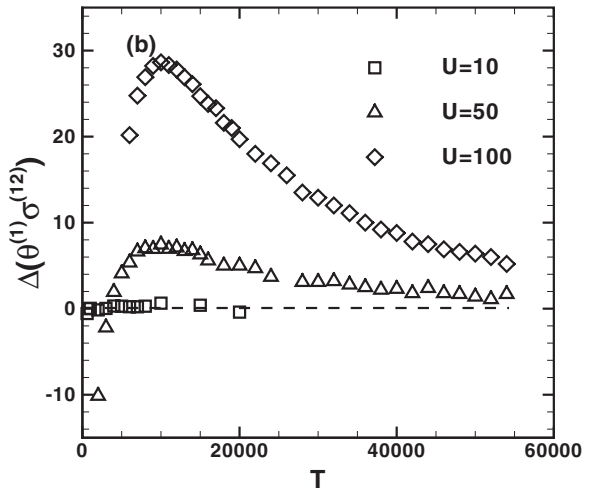

FIG. 11. Interspecies stress difference between the flow direction and the perpendicular directions as a function of granular temperature. $\theta^{(1)}=\theta^{(2)}=0.2$.

are close enough the Bernoulli effect on the spheres can significantly affect their motions. Similarly, if there is a nonuniform relative motion in the particulate system, the resulting stress difference could be important and could lead to particle segregation. Second, the relative motion between species enhances random velocity fluctuations (the granular temperature) and thus increases the magnitude of the stresses. As shown in Figs. 8 and 9, these stresses are quite sensitive to the granular temperature.

In many granular flow simulations, it is often reported that the stress component in the flow direction (x direction) is typically larger than the stress components in other directions. While this holds for the intraspecies stresses calculated in this paper; this is not always true for the interspecies stress. As plotted in Fig. 7, the magnitude of the interspecies stress in the directions perpendicular to the flow is larger than the magnitude of the stress in the flow direction, suggesting that particles of one species apply a significant force to push aside particles of the other species while passing each other. The stress difference between the flow direction and the perpendicular directions, $\sigma_{xx}-(\sigma_{yy}+\sigma_{zz})/2$, is plotted in Figs. 10 and 11 for intraspecies and interspecies interactions, respectively.

V. CONCLUSIONS

A series of direct numerical simulations is performed to study properties of species interaction force and stress tensors arising from the two-equation formulation [11] for binary particulate systems. To simplify our discussion in the present paper we present only results obtained in an idealized simple system. In the system, particles of the two species have the same mechanical properties. There are equal numbers of particles for both species. Their interactions are modeled by a linear force model without energy dissipation. Despite the simplicity of the system, the results show many interesting features of the stresses and the interaction force.

In the case of thermal equilibrium, where the two species undergo random fluctuations without relative mean motion, the relative contribution of the interspecies stress to the total mixture stress increases with the particle volume fraction and decreases with the granular temperature. In the limit of zero granular temperature, because there are equal numbers of particles for both the species and the force models for their interactions are the same, one can prove that the interspecies stress contributes half of the mixture stress.

When the two species undergo a relative motion, the drag force between the two species is proportional to the relative velocity for low Mach numbers. Relative motion also affects intraspecies and interspecies stresses. Its contribution to the stresses is quadratically proportional to the relative velocity. For many granular flows, the stress component in the flow direction is often larger than the stress components in the directions perpendicular to the flow. For the cases simulated in the present paper, this is always true for the intraspecies stress but true for the interspecies stresses only at low granular temperatures.

Finally, the authors would like to emphasize that the two-equation formulation for dense binary particulate systems is in an early stage of its development. We have only studied very limited systems in the present paper. Other effects, such as those dependent on the ratio of the volume fractions of the species, energy dissipation during particle interactions, and size ratio of the particles, have not been studied for two-equation formulations. The size ratio effect is especially important in the attempt to seek a unified mathematical description that is valid for problems ranging from molecular scale mixing to disperse multiphase flows.

ACKNOWLEDGMENTS

The author would like to acknowledge many important discussions with Dr. R. M. Rauenzahn and Dr. X. Ma. This work was performed under the auspices of the United States Department of Energy.

[1] J. M. Ottino and D. V. Khakhar, Annu. Rev. Fluid Mech. **32**, 55 (2000).
[2] C. Henrique, G. Batrouni, and D. Bideau, Phys. Rev. E **63**, 011304 (2000).
[3] M. G. Rasul, V. Rudolph, and M. Carsky, Powder Technol. **126**, 116 (2002).
[4] S. C. Yang, Powder Technol. **164**, 65 (2006).
[5] Y. Q. Feng, B. H. Xu, S. J. Zhang, and A. B. Yu, AIChE J. **50**, 1713 (2004).
[6] L. S. Lu and S. S. Hsiau, Powder Technol. **160**, 170 (2005).
[7] T. G. Elizarova, I. A. Graur, and J.-C. Lengrand, Eur. J. Mech. B/Fluids **20**, 351 (2001).
[8] J. M. Powers, Phys. Fluids **16**, 2975 (2004).
[9] A. J. Scannapieco and B. Cheng, Phys. Lett. A **299**, 49 (2002).

[10] L. S. Luo and S. S. Girimaji, Phys. Rev. E **67**, 036302 (2003).
[11] D. Z. Zhang, X. Ma, and R. M. Rauenzahn, Phys. Rev. Lett. **97**, 048301 (2006).
[12] J. H. Irving and I. G. Kirkwood, J. Chem. Phys. **18**, 817 (1950).
[13] D. Z. Zhang and A. Prosperetti, J. Fluid Mech. **267**, 185 (1994).
[14] D. Z. Zhang and A. Prosperetti, Int. J. Multiphase Flow **23**, 425 (1997).
[15] A. Prosperetti and G. Tryggvason, *Computational Methods for Multiphase Flow* (Cambridge University Press, Cambridge, U.K., 2006), Chap. 7.
[16] M. P. Allen and D. J. Tildesley, *Computer Simulation of Liquids* (Clarendon Press, Oxford, 1987).
[17] D. Z. Zhang and R. Rauenzahn, J. Rheol. **41**, 1275 (1997).
[18] D. Z. Zhang and R. Rauenzahn, J. Rheol. **44**, 1019 (2000).
[19] D. Z. Zhang, W. B. VanderHeyden, Q. Zou, and N. T. Padial-Collins, Int. J. Multiphase Flow **33**, 86 (2007).
[20] X. Ma and D. Z. Zhang, J. Mech. Phys. Solids **54**, 1426 (2006).
[21] D. Z. Zhang, Phys. Rev. E **71**, 041303 (2005).
[22] S. B. Savage, J. Fluid Mech. **92**, 53 (1979).
[23] S. B. Savage and D. J. Jeffrey, J. Fluid Mech. **110**, 255 (1981).
[24] T. D. Atkinson, J. Butcher, M. J. Izard, and R. M. Nedderman, Chem. Eng. Sci. **38**, 91 (1983).
[25] C. R. Wassgren, J. A. Cordova, R. Zenit, and A. Karion, Phys. Fluids **15**, 3318 (2003).
[26] I. Albert, P. Tegzes, R. Albert, J. G. Sample, A. L. Barabási, T. Vicsek, B. Kahng, and P. Schiffer, Phys. Rev. E **64**, 031307 (2001).
[27] C. Cercignani, *The Boltzmann Equation and Its Applications* (Springer, New York, 1988).
[28] A. Gopinath and D. L. Koch, Phys. Fluids **11**, 2772 (1999).
[29] Y. Feng, B. Xu, S. Zhang, and A. Yu, AIChE J. **50**, 1713 (2004).
[30] O. Zik, J. Stavans, and Y. Rabin, Europhys. Lett. **17**, 315 (1992).
[31] J. Geng and R. P. Behringer, Phys. Rev. E **71**, 011302 (2005).